HHS Public Access

Author manuscript

Curr Biol. Author manuscript; available in PMC 2020 February 04.

Published in final edited form as:

Curr Biol. 2019 February 04; 29(3): 449–460.e2. doi:10.1016/j.cub.2018.12.043.

The DNA damage checkpoint and the spindle position checkpoint maintain meiotic commitment in *Saccharomyces cerevisiae*

Olivia Ballew[1] and **Soni Lacefield**[1,2,*]

[1]Indiana University, Department of Biology, Bloomington, IN USA

[2]Lead contact

Summary

During meiosis, diploid progenitor cells undergo one round of DNA replication followed by two rounds of chromosome segregation to form haploid gametes. Once cells initiate the meiotic divisions, it is imperative that they finish meiosis. A failure to maintain meiosis can result in highly aberrant polyploid cells, which could lead to oncogenesis in the germline. How cells stay committed to finishing meiosis, even in the presence of a mitosis-inducing signal is poorly understood. We addressed this question in budding yeast, in which cells enter meiosis when starved. If nutrient-rich medium is added before a defined commitment point in mid prometaphase I, they can return to mitosis. Cells in stages beyond the commitment point will finish meiosis, even with nutrient addition. Because checkpoints are signaling pathways known to couple cell cycle processes with one another, we asked if checkpoints could ensure meiotic commitment. We find that two checkpoints with well-defined functions in mitosis, the DNA damage checkpoint and the spindle position checkpoint, have crucial roles in meiotic commitment. With nutrient-rich medium addition at stages beyond the commitment point, cells which are deficient in both checkpoints because they lack Rad53 and either Bub2, Bfa1, or Kin4, can return to mitotic growth and go on to form polyploid cells. The results demonstrate that the two checkpoints prevent cells from exiting meiosis in the presence of a mitosis-inducing signal. This study reveals a previously unknown function for the DNA damage checkpoint and the spindle position checkpoint in maintaining meiotic commitment.

Graphical Abstract

Ballew and Lacefield show that two checkpoint pathways, the canononical DNA damage checkpoint and the spindle position checkpoint, are required to maintain meiotic commitment. In

*corresponding author: Soni Lacefield, Indiana University, 1001 E. Third St., Jordan Hall A315, Bloomington, IN 47405, Phone: 812-856-2429, Fax: 812-855-1687, sonil@indiana.edu.

Author Contributions

O.B. and S.L. designed the experiments, performed the experiments, analyzed the data, and wrote the manuscript.

Declaration of Interests

The authors do not have any competing interests to declare.

the presence of a mitosis-inducing signal, cells that lack both checkpoints exit meiosis inappropriately and become polyploid.

Keywords

meiosis; mitosis; DNA damage checkpoint; spindle position checkpoint; return-to-growth; meiotic commitment

Introduction

Meiosis is a cell division pathway which is distinct from the mitotic pathway. During meiosis, diploid cells undergo one round of DNA replication followed by two rounds of chromosome segregation, in which homologous chromosomes segregate in meiosis I and sister chromatids segregate in meiosis II. The haploid meiotic products then differentiate into gametes. During mitosis, DNA replication is followed by chromosome segregation to produce two cells with equal ploidy. Distinct signals induce either meiosis or mitosis. It is currently unclear how meiotic cells remain committed to meiosis in the presence of a mitosis-inducing signal.

Many eukaryotic organisms, including humans, mice, frogs, flies, worms, and yeast have irreversible transition points at the end of prophase I or in prometaphase I in which they commit to undergoing the meiotic divisions [1–4]. For example, human and mouse oocytes arrest at prophase I and only resume meiosis and commit to finishing meiosis I upon hormone stimulation [2, 3]. In budding yeast, commitment can be assessed based on the cells response to nutrients [1]. Cells enter meiosis when starved of nitrogen and carbon. After entrance into meiosis, cells can return to mitosis in a process called return-to-growth (RTG) if nutrient-rich medium is provided before a defined commitment point in mid-prometaphase I [5–10]. Cells in stages beyond the meiotic commitment point complete meiosis even with nutrient addition. How budding yeast cells transition from an uncommitted state in which they can return to mitosis to a committed state in which they stay in meiosis is unknown.

Here, we use budding yeast to address how cells commit to meiosis in prometaphase I. Because checkpoint mechanisms couple cell cycle processes with one another, we asked if the meiotic checkpoint network (MCN) or the canonical DNA damage checkpoint were important for meiotic commitment. The MCN is a network of signaling mechanisms, which detects DNA double strand breaks (DSBs) and coordinates events in prophase I [11]. Approximately 150–200 programmed DSBs occur in prophase I to initiate meiotic recombination. Repair of those breaks is tightly coordinated to prevent the formation of gametes with genome damage [12, 13]. In contrast, the canonical DNA damage checkpoint, which arrests mitotic cells in metaphase in the presence of DNA damage, does not activate a DNA damage checkpoint delay in metaphase I; however, it can elicit a metaphase II delay [14]. Whether either of these checkpoint mechanisms coordinate meiotic commitment with meiotic progression is unknown.

The MCN and the canonical DNA damage checkpoint use many of the same components, including sensor kinases ATR and ATM (Mec1 and Tel1 in budding yeast, respectively), that bind damaged DNA, recruit repair enzymes, and signal the checkpoint [11, 15]. In the MCN, Mec1 and Tel1 activate Mek1, a meiosis-specific effector kinase, which delays cells in prophase I to provide time for repair [11]. In the canonical DNA damage checkpoint, Mec1 and Tel1 signal the effector kinase Rad53, which stabilizes securin (Pds1 in budding yeast) and down-regulates CDK activity to delay cells in metaphase [16–20]. The current model for why the canonical DNA damage checkpoint does not delay meiosis I is that Rad53 cannot easily access recombination sites and that protein phosphatase 4 keeps Rad53 inactive [14, 21]. Therefore, the MCN monitors DNA damage in meiosis I and the canonical DNA damage checkpoint monitors DNA damage in meiosis II.

We report the first characterization of the DNA damage checkpoint in RTG and meiotic commitment. We found that Mec1-deficient cells undergo an aberrant division upon nutrient-addition in mid-prometaphase I: cells underwent anaphase I and then budded. This phenotype also occurred in Rad53-deficient cells suggesting that the DNA damage checkpoint was required for meiotic commitment in prometaphase I. Further analysis demonstrated that the DNA damage checkpoint and the spindle position checkpoint are required for meiotic commitment beyond prometaphase I. Surprisingly, cells lacking both checkpoints failed to remain committed to meiosis and returned to mitosis from stages beyond the commitment point, creating polyploid cells. The function of the spindle position checkpoint was previously described in mitosis. Although it may not be a checkpoint in the classical definition, components Bub2 and Bfa1 inhibit the mitotic exit network when both spindle pole bodies (SPBs) are in the mother cell [22–25]. Once one SPB enters the bud, the mitotic exit network is activated. In meiosis I, the mitotic exit network is not activated and the spindle position checkpoint does not have an important role [26]. Our results demonstrate new functions for both the DNA damage checkpoint and the spindle position checkpoint in ensuring meiotic commitment.

Results:

Mec1 prevents the formation of polyploid cells after nutrient-rich medium addition

To address whether the DNA damage checkpoint coordinates the transition to meiotic commitment within prometaphase I, we asked if ablating the checkpoint caused a timing defect in commitment. We deleted *MEC1*, which encodes a DNA damage checkpoint kinase [27]. Because *MEC1* is essential, we also deleted *SML1*, which suppresses *mec1Δ* lethality [28]. We used microfluidics to analyze commitment by introducing nutrient-rich medium at specific time points. To identify the meiotic stages, we monitored cells with multiple genetically encoded fluorescent markers. Zip1-GFP allowed us to identify prophase I because Zip1 is a component of the synaptonemal complex, which assembles and disassembles in prophase I [29, 30]. The alpha-tubulin, GFP-Tub1, which incorporates into microtubules, along with Spc42-mCherry, a SPB component, allowed us to measure spindle length to differentiate prometaphase I, metaphase I, and anaphase I [8, 31]. We defined the prometaphase I onset as the initial separation of SPBs [8]. As cells progress through

prometaphase I to metaphase I, the spindle elongates to 3.5 μm. Further elongation of the spindle occurs in anaphase I.

As expected from our previous study, wildtype cells committed to meiosis in midprometaphase I (Figure 1A–D) [8]. Cells in late prometaphase I upon nutrient addition finished meiosis (Figure 1B, 1D). Cells in early prometaphase I underwent RTG (Figure 1C, 1D). We found that *mec1Δ sml1Δ* cells, like wildtype cells, committed to meiosis in prometaphase I, with some cells that underwent RTG and some cells that finished meiosis upon addition of rich medium (Figure 1E). To ensure that we were accurately staging the *mec1Δ sml1Δ* cells, we monitored a separase biosensor and showed that separase cleaved the meiosis-specific cohesin subunit Rec8 at anaphase I spindle elongation, as in wildtype cells [32] (Figure S1A–B).

In addition, *mec1Δ sml1Δ* cells displayed two novel phenotypes upon nutrient addition in prometaphase I (Figure 1E–G). We rarely observed these phenotypes upon nutrient addition at other stages. For ease of discussion, we are calling them class I and class II phenotypes. We further characterized the two phenotypes to determine how they differ.

Class I cells underwent anaphase 38 ± 5 mins after nutrient addition, budded, and then repositioned one of the SPBs into the bud, resulting in correct distribution of one nucleus in the mother and one in the bud (average ± SE; Figure 1F). This phenotype is aberrant because normally cells that underwent RTG from prometaphase I initiated anaphase after bud formation (Figure 1C)[8]. 5% of cells in prometaphase I displayed the class I phenotype upon nutrient addition (Figure 1E). Mother and daughter cells often underwent 1–2 more divisions after the aberrant division, suggesting that they were viable. In this class, we also included a small population of cells that underwent anaphase with similar timing, budded, but then arrested (Figure S1C).

Class II cells had a more severe phenotype. The cells underwent anaphase 24 ± 3 mins after nutrient addition, the SPBs duplicated and two spindles formed (average ± SE). The cells then budded and divided both nuclei, creating a multi-nucleate mother cell, as assessed by formation of multiple spindles (Figure 1G). These results were surprising because they suggested that Mec1 and Sml1 prevent the formation of polyploid cells after nutrient-rich medium addition in prometaphase I. These cells often undergo another division after the aberrant division, suggesting that they are viable. 12% of *mec1Δ sml1Δ* cells in prometaphase I displayed this phenotype upon nutrient addition (Figure 1E).

Cells that displayed class I and class II phenotypes were in mid-prometaphase I upon nutrient addition. As cells progressed through prometaphase I, the spindle elongated from the initial separation of the SPBs until 3.5 μm in metaphase I [8]. In wildtype cells, the commitment point was in mid-prometaphase I, such that cells with shorter prometaphase I spindles (1.8 ± 0.1 μm) underwent RTG and those with longer prometaphase I spindles (2.5 ± 0.1 μm) finished meiosis (average ± SE; Figure 1H). The *mec1Δ sml1Δ* cells that displayed aberrant phenotypes were in mid-prometaphase I when nutrient-rich medium was added and had an average spindle length of 2.3 ± 0.1 μm (Figure 1I). There was not a significant difference in average spindle length among class I and class II phenotypes

(Figure S1D). These results demonstrated that cells in mid-prometaphase I required a DNA damage checkpoint delay to prevent premature chromosome segregation.

The DNA damage checkpoint is required at the time of nutrient-rich medium addition to prevent the formation of polyploid cells

Mec1 is upstream of both the effector kinase Rad53 in the canonical DNA damage checkpoint and the meiosis-specific effector kinase Mek1 in the MCN [11]. To determine which of these two pathways prevented the class I and class II phenotypes, we monitored *rad53Δ sml1Δ* and *mek1Δ* cells during commitment and RTG. Similar to *mec1Δ sml1Δ* cells, a proportion of *rad53Δ sml1Δ* cells displayed class I and class II phenotypes with nutrient-rich medium addition in prometaphase I (Figure 1J). In contrast, the *mek1Δ* cells and *sml1Δ* cells did not display class I or class II phenotypes (Figure 1J). Therefore, the results suggested that Mec1 signaled through the Rad53 checkpoint pathway to prevent premature segregation upon nutrient addition in prometaphase I. This was surprising because previous studies showed that Rad53 does not activate the DNA damage checkpoint in meiosis I [14].

Mec1 also has roles in DNA damage signaling during premeiotic S phase and prophase I [11]. Therefore, we wanted to determine if Mec1 function was required during meiosis or the transition back to mitosis after nutrient addition. To distinguish between these two possibilities, we used a technique called anchor away to rapidly remove Mec1 from the nucleus upon rapamycin addition [33]. Mec1 was tagged with FRB and RPL13A was tagged with FKBP12. Mec1-FRB is rapidly depleted from the nucleus into the cytosol with addition of rapamycin due to the formation of a stable interaction with RPL13A-FKBP12, a ribosomal protein imported into the nucleus to assemble with rRNAs and then exported back to the cytoplasm. Mec1-FRB cells sporulated and produced viable spores when rapamycin was absent, suggesting that the tag did not cause major defects in Mec1 function. With rapamycin addition at meiosis initiation, spores were inviable, a phenotype similar to *mec1Δ sml1Δ* cells, suggesting Mec1 was depleted from the nucleus (data not shown).

To dissect the role of Mec1 in RTG, we allowed Mec1 function during premeiotic S phase and prophase I, and then depleted Mec1 at prophase I exit by adding rapamycin. We then added nutrient-rich medium in prometaphase I. Similar to *mec1Δ sml1Δ* cells, 21% of cells that underwent RTG with Mec1 depleted displayed either class I or class II phenotypes (Figure 1K). Only 5% of cells displayed class I or class II phenotypes without rapamycin, suggesting that the tag caused only a minor defect in Mec1 function. Overall, our results demonstrate that class I and class II phenotypes are due to loss of Mec1 at nutrient addition, not during S phase or prophase I. In conclusion, our results showed that the DNA damage checkpoint prevents aberrant segregation and polyploidy upon nutrient addition in prometaphase I.

DSBs Signal the DNA damage checkpoint during RTG and commitment from prometaphase I

The findings that *mec1Δ sml1Δ* cells undergo aberrant phenotypes led us to ask whether there was residual DNA damage that signaled the checkpoint in prometaphase I after

nutrient addition. Although the MCN should ensure that DNA damage is repaired prior to prophase I exit, we asked if some cells entered the meiotic divisions with persistent DNA damage. Past studies using populations of cells indicated that as cells exit pachytene, recombination intermediates at certain hotspots are resolved, with cross-over products appearing in late prophase I [34, 35]. Because this timing is in close proximity to prometaphase I, we hypothesized that by monitoring individual cells, we might detect cells with unrepaired DSBs during prometaphase I. We performed time-lapse microscopy of meiosis in cells expressing Rad52-GFP and Spc42-mCherry. Rad52 functions in early and late steps of meiotic DSB repair, loading Rad51 filaments onto RPA-coated single-stranded DNA and annealing DSB ends in crossover and noncrossover pathways [36, 37], making it an excellent marker to study DSB repair [38].

Using time-lapse microscopy, we monitored normal meiosis and found that 38% of cells had at least one Rad52-GFP focus that persisted into prometaphase I (Figure 2A–C). We expected a greater number of cells without foci due to the MCN's role in delaying cells with unrepaired DNA damage in prophase I [11]. Interestingly, 61% of cells with Rad52-GFP foci in prometaphase I had at least one Rad52-GFP focus that persisted through both meiotic divisions (Figure 2A). Furthermore, most Rad52-GFP foci present in prometaphase I were dependent on Spo11, the enzyme that makes programmed DSBs in prophase I [39]. Only 5% of *spo11Δ* cells had Rad52-GFP foci that persisted into prometaphase I (Figure 2C), consistent with a previous study that found few Rad52-GFP foci in prophase I in *spo11Δ* cells [38]. These results demonstrated that programmed DSBs are repaired in stages beyond prometaphase I.

Previous studies showed that cells with persistent DNA damage due to mutations in genes required for programmed DSB repair did not have a canonical DNA damage checkpoint delay in metaphase I [14, 15]. Consistent with these studies, we found that cells with Rad52-GFP foci that persisted into the meiotic divisions did not show a delay in metaphase I duration (Figure 2D). In metaphase II, cells with Rad52-GFP foci had an 11-minute delay compared to cells without Rad52-GFP foci (Figure 2E).

We next asked if cells that underwent RTG or committed to finishing meiosis from prometaphase I activated the DNA damage checkpoint in response to unrepaired meiotic programmed DSBs. We used microfluidics to introduce nutrient-rich medium and assessed whether the cells in prometaphase I underwent RTG or meiosis (Figure 3A–B). The addition of nutrients did not increase the number of cells with Rad52-GFP foci; 38% of cells had Rad52-GFP foci, which were present prior to nutrient addition (Figure 3C, 2C). Cells with Rad52-GFP foci had an average time from nutrient addition at prometaphase I to the mitotic anaphase of 247 ± 8 mins, which was 30 mins slower than cells without foci at 218 ± 4 mins (average ± SE; Figure 3D). The cells with and without Rad52-GFP foci budded with similar timing, approximately 170 mins after nutrient addition, suggesting that the delay occurred after bud formation (Figure 3E).

We imaged *mec1Δ sml1Δ* cells to determine if the delay depended on the DNA damage checkpoint. Because Mec1 is also involved in repair of DNA DSBs [11], 97% of *mec1Δ sml1Δ* double mutants had Rad52-GFP foci as they underwent RTG, which is similar to

mec1Δ sml1Δ mutants that had persistent Rad52-GFP foci in a normal meiosis (Figure 3C, 2C). The *mec1Δ sml1Δ* cells underwent mitotic anaphase 215 ± 11 mins after nutrient addition in prometaphase I, similar to wildtype cells without Rad52-GFP foci (average ± SE; Figure 3D). These results suggest that as cells transitioned from prometaphase I to mitosis, the DNA damage checkpoint delayed anaphase onset when residual meiotic DNA damage was present.

We measured time from nutrient-rich medium addition in prometaphase I to anaphase I and II in committed cells that stayed in meiosis. Remarkably, cells with Rad52-GFP had a 23-minute delay to anaphase I onset when compared to cells without Rad52-GFP foci, with the time from nutrient addition to anaphase onset at 56 ± 5 mins compared to 33 ± 2 mins, respectively (average ± SE; Figure 3F). The *mec1Δ sml1Δ* mutants with Rad52-GFP foci underwent anaphase I in 44 ± 4 mins, suggesting that the delay depended on the DNA damage checkpoint. Anaphase II was delayed by 26 mins in cells with Rad52-GFP foci and this delay was absent in *mec1Δ sml1Δ* cells (Figure 3G). The metaphase I delay in committed cells was unexpected because previous studies showed that cells with persistent DNA damage did not have a DNA damage checkpoint delay in metaphase I, but did have a delay in metaphase II [14, 15]. These results demonstrate that the DNA damage checkpoint was activated in meiosis I and meiosis II in committed cells with addition of nutrient-rich medium.

The *mec1Δ sml1Δ* cells that underwent an aberrant class II segregation initially underwent a reductional division.

We further characterized *mec1Δ sml1Δ* cells that displayed the aberrant phenotypes. We asked if the division prior to bud formation was a meiosis I-like division, in which homologous chromosomes segregated, or a mitotic-like division in which sister chromatids separated. We tagged one homologous chromosome IV with a LacO array near the centromere in cells expressing GFP-LacI [40]. Cells that underwent a normal RTG in prometaphase I separated sister chromatids, resulting in one GFP focus in the mother and one focus in the daughter cell (Figure 4A). Committed cells that finished meiosis after nutrient-rich medium addition segregated homologous chromosomes in meiosis I, with one GFP focus at one of the two SPBs. In meiosis II, sister chromatids separated, with a GFP focus at two of the four SPBs (Figure 4B).

The class I and class II cells showed one GFP focus at one of the two SPBs, suggesting that homologous chromosomes segregated, as in meiosis I (Figure 4C, D). Interestingly, in class I cells, the SPBs came back together after spindle elongation and then separated again, positioning one SPB in the daughter cell (Figure 4C). After the second separation, GFP foci were present at both SPBs. These results made us question whether the initial segregation was of homologous chromosomes or whether monopolar attachments caused premature spindle elongation in the class I cells. We tagged both homologs with LacO and monitored GFP-LacI. 50% of cells had GFP foci at each SPB as though homologs segregated. 40% of cells had GFP foci at only one SPB, suggesting that the homologs mis-segregated. 10% of cells had at least one GFP focus between separated SPBs (Figure S1E). When the SPBs came back together, the GFP foci re-oriented and segregated to both poles. These results

suggested that class I cells underwent an abnormal spindle elongation in which some homologous chromosomes segregated and some monopolar attachments were made, but then the attachments were corrected and sister chromatids segregated.

In contrast, the class II cells initially segregated homologs and then assembled two spindles, formed a bud, and then separated sister chromatids to create a multi-nucleate polyploid mother cell (Figure 4D). We did not see additional GFP foci, suggesting the DNA did not replicate between the two divisions. The data suggest that class II mutants underwent meiosis I, initiated metaphase II, then exited meiosis and entered mitosis from metaphase II.

Cdc14 is fully released in anaphase I in class II *mec1*Δ *sml1*Δ cells

Our results demonstrate that class I and class II cells both underwent an anaphase I spindle elongation before budding but then gave distinct chromosome segregation phenotypes. We speculated that a major difference depended upon Cdc14 release at anaphase I. In mitosis, Cdc14 phosphatase is held in the nucleolus until its step-wise release in anaphase [41]. Once released, Cdc14 reverses the phosphorylation of Cdk1 substrates to allow mitotic exit and cytokinesis. Cdc14 is also essential for meiosis, where it is released from the nucleolus in anaphase I, re-sequestered, and re-released in anaphase II [42, 43].

We tagged Cdc14 with GFP in cells with Spc42-mCherry to determine the stage Cdc14-GFP was released in *mec1Δ sml1Δ* cells. We monitored cells in which nutrient-rich medium was added in prometaphase I. In cells that underwent a normal RTG, Cdc14-GFP was released from the nucleolus upon anaphase spindle elongation (Figure 5A). In cells committed to meiosis, Cdc14-GFP was released in anaphase I, re-sequestered, and released again in anaphase II, similar to a normal meiosis (Figure 5B).

In the class I *mec1Δ sml1Δ* cells, Cdc14-GFP was not released from the nucleolus during the premature spindle elongation but instead was released after the cell budded, reoriented its spindle, and then positioned one nucleus into the bud (Figure 5C, intensity measurements in Figure S2). Because our time-lapse images are taken every 10mins, we cannot exclude the possibility that Cdc14-GFP was partially and quickly released and re-sequestered. However, our results supported our hypothesis that restraining Cdc14 prevented cells from exiting until one nucleus was properly positioned into the daughter cell.

In class II *mec1Δ sml1Δ* cells, Cdc14-GFP was released from the nucleolus at anaphase I. Cdc14-GFP was then re-sequestered into the nucleolus and then released again after the cell budded and underwent anaphase across the bud neck (Figure 5D). The data suggest that the class II cells underwent meiosis I, initiated meiosis II, and then began a mitotic cell cycle in which they budded, segregated sister chromatids, and then released Cdc14-GFP again. In conclusion, our results demonstrated that class I and II cells differed in the timing of Cdc14 release with respect to spindle elongation.

The DNA damage checkpoint and the spindle position checkpoint ensure meiotic commitment

The finding that class I cells did not fully release Cdc14 during anaphase I, but instead only after the cell budded and positioned one nucleus into the daughter cell suggested that another

mechanism may play a role in ensuring that chromosomes segregated into mother and daughter cells before mitotic exit. In mitotic cells, the spindle position checkpoint inhibits the mitotic exit network and full Cdc14 release when the spindle is mis-positioned. The inhibitory activity of spindle position checkpoint components ensure that Cdc14 is not fully released and cells do not exit mitosis until one SPB is positioned in the bud [25, 44, 45]. However, in meiosis, both divisions occur in the mother and Cdc14 release does not depend on spindle position. Furthermore, the mitotic exit network does not function in meiosis I and the spindle position checkpoint does not have a known role in meiosis [46].

We hypothesized that the spindle position checkpoint prevented full Cdc14 release in class I cells until the anaphase spindle was correctly positioned into the bud. This hypothesis led to the prediction that, without the spindle position checkpoint, class I cells would release Cdc14 with anaphase I spindle elongation, like class II cells. We tested this notion in *rad53Δ sml1Δ* cells instead of *mec1Δ sml1Δ* cells because the percent of class I cells is modestly higher in the former (Figure 1J). We deleted *BUB2*, which encodes a protein that prevents Cdc14 release until the spindle is properly oriented with one SPB in the bud [44]. We monitored *rad53Δ sml1Δ bub2Δ* cells after nutrient-rich medium addition in prometaphase I; none of these cells displayed the class I phenotype (Figure 6A). Instead, 17% of prometaphase I cells displayed the class II phenotype: cells underwent anaphase I, duplicated SPBs, then budded, and underwent a mitotic division with two spindles. Only 2% of *bub2Δ* cells showed this phenotype (Figure 6B). Significantly, the combined number of cells with the class I and II phenotype in *rad53Δ sml1Δ* cells was also 17% (Figure 1J, 6C). These results suggest that the class I phenotype was converted to the class II phenotype by deletion of *BUB2*. Therefore, the spindle position checkpoint prevented polyploidy in class I *rad53Δ sml1Δ* cells by preventing full Cdc14 release, allowing cells to bud and position one nucleus into the bud prior to exiting the cell cycle.

6% of *rad53Δ sml1Δ bub2Δ* cells also showed a spindle position defect during RTG (Figure 6A, S3A). This phenotype was distinct from that of class I and II cells because anaphase occurred after bud formation, as it does in a normal RTG. However, anaphase occurred in the mother cell and one nucleus was not reoriented into the daughter cell prior to mitotic exit. Therefore, Bub2 also prevented spindle position defects in *rad53Δ sml1Δ* cells that underwent RTG.

Surprisingly, *rad53Δ sml1Δ bub2Δ* cells also displayed an uncommitted phenotype when nutrients were added in metaphase I or anaphase I, stages beyond the meiotic commitment point. 29% of *rad53Δ sml1Δ bub2Δ* cells failed to stay committed in metaphase I and 34% failed to stay committed in anaphase I (Figure 6A). After undergoing anaphase I, the uncommitted cells duplicated SPBs, budded and divided one nucleus in the mother cell and one across the bud neck, resulting in a mother cell that is polyploid and multi-nucleate, as determined by formation of multiple spindles (Figure S3B). This phenotype only occurs when nutrient-rich medium is added and does not occur in our microfluidics device when nutrient-poor sporulation medium was added (Figure S3C). Wildtype cells in metaphase I and anaphase I are committed to meiosis and will finish meiosis and form spores ([8]; Figure 1D). *bub2Δ* cells did not show a major commitment defect, with only 6% of metaphase I and

3% of anaphase I cells failing to stay committed to meiosis (Figure 6B). *rad53Δ sml1Δ* cells showed 9% uncommitted cells in metaphase I and 5% in anaphase I (Figure 6C).

To ensure this phenotype is dependent on the spindle position checkpoint, and not a different Bub2 function, we analyzed several other strains. We asked if other spindle position checkpoint components showed this defect by analyzing *rad53Δ sml1Δ bfa1Δ* cells and *rad53Δ sml1Δ kin4Δ* cells. In mitosis, Bfa1functions with Bub2 as GTPase activating proteins to keep the GTPase Tem1 inactive, inhibiting full Cdc14 release [41, 44, 47, 48]. Kin4 functions upstream of Bub2-Bfa1 and is essential for inhibition of Cdc14 release [23, 24]. Both *rad53Δ sml1Δ bfa1Δ* cells and *rad53Δ sml1Δ kin4Δ* mutants showed a commitment defect when nutrient-rich medium was added to the cells in metaphase I and anaphase I (Figure 6D–F). In contrast to the *rad53Δ sml1Δ bub2Δ* cells, there were no bud defects or spindle position defects. Similar to *bub2Δ,* the *bfa1Δ* and *kin4Δ* cells only had a minor commitment defect, singularly (Figure 6G–H). Bub2 is also involved in spindle checkpoint signaling [49]. However, deletion of spindle checkpoint component Mad3 combined with the loss of the DNA damage checkpoint did not show an uncommitted phenotype in stages beyond prometaphase I (Figure S3D–E). In conclusion, our results suggest that this surprising uncommitted phenotype was dependent on loss of both the DNA damage and the spindle position checkpoints, not a different function of Bub2.

Discussion

Our results demonstrate that the canonical DNA damage checkpoint and the spindle position checkpoint, which do not have major functions in meiosis I, are required for maintenance of meiotic commitment. Cells lacking both checkpoints failed to maintain commitment upon rich medium addition and exited meiosis inappropriately, causing polyploidy. We propose that addition of nutrient-rich medium allows the cellular changes needed to promote the DNA damage and spindle position checkpoints. They are likely sensing the signal that activates them in mitosis: residual DNA damage for DNA damage checkpoint signaling and spindle mis-position for spindle position checkpoint activity. Together the two checkpoints maintain meiotic commitment by preventing cells from exiting meiosis after anaphase I, which allows cells to continue through meiosis II and gametogenesis.

Interestingly, neither the DNA damage checkpoint nor the spindle position checkpoint pathway is utilized during meiosis I. Previous studies have shown that the DNA damage checkpoint does not delay meiosis I progression in the presence of meiosis-specific or exogenously induced DNA damage [14, 15]. By monitoring Rad52-GFP, a protein involved in DSB repair, we surprisingly found that approximately 40% of cells had residual DNA damage as they entered the meiotic divisions. These cells did not have a DNA damage checkpoint delay in a normal meiosis I. However, with addition of nutrient-rich medium, the DNA damage checkpoint delayed cells with Rad52-GFP foci in metaphase I. We hypothesize that the DNA damage checkpoint is activated by residual DSBs and this activity delays securin degradation and Cdc14 release, as it does in mitosis [16–20]. We propose that the delay prevents cells in mid-prometaphase I from undergoing anaphase I prematurely and exiting meiosis inappropriately.

The spindle position checkpoint is also not active in a normal meiosis I [46]. In mitosis, the spindle position checkpoint proteins Bub2 and Bfa1 localize to SPBs and inhibit the mitotic exit network to prevent full Cdc14 release [25, 44, 45]. When the spindle is positioned into the bud, the mitotic exit network is now activated for cells to exit mitosis. In meiosis I, cells do not have a bud, the mitotic exit network is not active, and some of the signaling proteins are not localized on SPBs. We propose that addition of nutrient-rich medium promotes activation of the mitotic exit network. Cells stay committed to meiosis because the spindle position checkpoint and the DNA damage checkpoint prevent full Cdc14 release and cells continue into meiosis II. We propose that the loss of both spindle position and DNA damage checkpoints, could lead to a full Cdc14 release through the mitotic exit network and cause cells to exit meiosis after anaphase I and return to mitosis. Overall, this analysis highlights the importance of these checkpoint pathways in ensuring that cells maintain meiotic commitment and prevent polyploidy in the presence of a mitosis-inducing signal.

STAR METHODS

CONTACT FOR REAGENT AND RESOURCE SHARING

Further information and requests for resources and reagents should be directed to and will be fulfilled by the Lead Contact, Soni Lacefield (sonil@indiana.edu).

EXPERIMENTAL MODEL AND SUBJECT DETAILS

Budding Yeast Methods—Strains used in this study are derivatives of *S. cerevisiae* W303. Strains are described in Table S1. Gene deletions and tagging were made using standard PCR-based transformation methods (Table S2) [50]. ZIP1 was tagged with GFP as described. Plasmids containing *GFP-TUB1*, *mCherry-TUB1, LacO,* and *CUP1pr-LacI* were integrated into the genome [31, 40]. Gene deletions in a *mec1*Δ or *rad53*Δ background were crossed in.

For RTG experiments, cells were grown in YPD (1% bacto-yeast extract, 2% bactopeptone, 2% glucose) at 30°C, transferred to YPA (1% yeast extract, 2% bactopeptone, 1% potassium acetate) for 12 hours at 30°C, washed once with 1% potassium acetate, and then incubated in 1% potassium acetate at 25°C for 8 hours. Cells were then loaded into microfluidics chambers (CellAsic Y04D yeast perfusion plates). Once loaded, 1% potassium acetate was flowed through for an additional 20–60 minutes depending on cell cycle progression. 2X synthetic complete (SC) medium (0.67% bacto-yeast nitrogen base without amino acids, 0.2% dropout mix with all amino acids, 2% glucose) was then flowed through the chamber to induce return-to-growth. For anchor away experiments, once cells were loaded into microfluidics chambers, 1% potassium acetate containing 1 μg/mL of rapamycin was flowed through the chamber for 30 minutes, and then SC containing 1 μg/mL of rapamycin was then flowed into chamber to induce return-to-growth. For RTG experiments using strain LY6220, 15 μM of $CuSO_4$ was added when cells were transferred to 1% potassium acetate.

For meiosis experiments, once cells were loaded into microfluidics chambers, 1 % potassium acetate was flowed through for 12 hours.

METHOD DETAILS

Microscope Image Acquisition and Time-lapse Microscopy—Cells were imaged using a Nikon Ti-E inverted microscope equipped with a 60X oil objective (PlanApo 1.4NA), a Lambda 10–3 optical filter changer and smartshutter (Sutter instrument), GFP and mCherry filters (Chroma Technology), Cool- SNAPHQ2 CCD camera (Photometrics), and the ONIX microfluidics system (Millipore). Z-stacks of 5× 1.2 mm sections were acquired in 10 minute intervals for 12 hours with exposure times of 60–70 ms for Brightfield and 700–900 ms for GFP and mCherry. Z- stacks were combined into a single maximum intensity projection with NIS-Elements software (Nikon).

Experiments using LY 6124 (GFP-Rec8) were imaged using a DeltaVision Elite equipped with an Olympus 60X oil objective (PlanApo 1.4 NA), a sCMOS Edge 5.5 camera, World Precision Instruments Environmental Chamber, and SoftWorx imaging software. Cells were loaded on a coverslip and under an agar pad containing potassium acetate.

QUANTIFICATION AND STATISTICAL ANALYSIS

Spindle Measurement—The spindle length was measured by using the NIS line tool and drawing a straight line between spindle pole bodies on maximum projection in X and Y. The distance between spindle pole bodies was then measured in Z. Spindle length was then calculated by inputting XY measurement and Z measurement into the Pythagorean theorem equation.

Fluorescence Intensity—Cdc14 fluorescence intensity was measured using ImageJ (FIJI) software. A circle was drawn in the Cdc14-GFP region and the mean intensity value was recorded. Another circle was drawn in a region not containing Cdc14-GFP and the mean intensity value was recorded. The difference of the two values was calculated and recorded to account for background fluorescence. The time of Cdc14-GFP release was also recorded. All difference values at each indicated stage were averaged together and plotted using Prism (GraphPad Software).

Statistical Analysis—All statistical analyses were performed using Prism (GraphPad Software). Statistical analysis of bud formation timing, anaphase onset timing, and spindle length was done using an unpaired, nonparametric Mann-Whitney test with computation of two-tailed exact p-values. Statistical analysis of percentage of outcome upon nutrient addition (Figure 1J, 1K, 6D–E, 6G–H) was entered into an rx contingency table. Compared data were entered into grouped-format tables with individual data values entered into subcolumns. Exact numbers were entered. The number of data points (n) is indicated in the figure legends. To analyze the Rad52-GFP foci percentages, and Rec8-GFP percentages, we used the two-sided Fisher's exact test. Percentages were computed in Excel spreadsheets (Microsoft) and then entered into Prism rx contingency tables. The number of cells (n) analyzed in every experiment is indicated in the figure legends. Difference among compared data was considered statistically significant if the p-value was <0.05 and is indicated with an asterisk.

Supplementary Material

Refer to Web version on PubMed Central for supplementary material.

Acknowledgements

We are grateful to David Quintana and Andreas Hochwagen for strains and constructs. We thank Frank Solomon and the Lacefield lab for insightful comments on the manuscript. This work was supported by an NIH grant (GM105755).

References

1. Winter E (2012). The Sum1/Ndt80 transcriptional switch and commitment to meiosis in Saccharomyces cerevisiae. Microbiol Mol Biol Rev 76, 1–15. [PubMed: 22390969]
2. Page AW, and Orr-Weaver TL (1997). Stopping and starting the meiotic cell cycle. Curr Opin Genet Dev 7, 23–31. [PubMed: 9024631]
3. Nebreda AR, and Ferby I (2000). Regulation of the meiotic cell cycle in oocytes. Curr Opin Cell Biol 12, 666–675. [PubMed: 11063930]
4. Kimble J (2011). Molecular regulation of the mitosis/meiosis decision in multicellular organisms. Cold Spring Harb Perspect Biol 3, a002683. [PubMed: 21646377]
5. Sherman F, and Roman H (1963). Evidence for two types of allelic recombination in yeast. Genetics 48, 255–261. [PubMed: 13977170]
6. Ganesan AT, Holter H, and Roberts C (1958). Some observations on sporulation in Saccharomyces. C R Trav Lab Carlsberg Chim 31, 1–6. [PubMed: 13639529]
7. Simchen G, Pinon R, and Salts Y (1972). Sporulation in Saccharomyces cerevisiae: premeiotic DNA synthesis, readiness and commitment. Exp Cell Res 75, 207–218. [PubMed: 4564471]
8. Tsuchiya D, Yang Y, and Lacefield S (2014). Positive feedback of NDT80 expression ensures irreversible meiotic commitment in budding yeast. PLoS Genet 10, e1004398. [PubMed: 24901499]
9. Friedlander G, Joseph-Strauss D, Carmi M, Zenvirth D, Simchen G, and Barkai N (2006). Modulation of the transcription regulatory program in yeast cells committed to sporulation. Genome Biol 7, R20. [PubMed: 16542486]
10. Tsuchiya D, and Lacefield S (2013). Cdk1 modulation ensures the coordination of cell-cycle events during the switch from meiotic prophase to mitosis. Current biology : CB 23, 1505–1513. [PubMed: 23871241]
11. Subramanian VV, and Hochwagen A (2014). The meiotic checkpoint network: step-by-step through meiotic prophase. Cold Spring Harb Perspect Biol 6, a016675. [PubMed: 25274702]
12. Buhler C, Borde V, and Lichten M (2007). Mapping meiotic single-strand DNA reveals a new landscape of DNA double-strand breaks in Saccharomyces cerevisiae. PLoS Biol 5, e324. [PubMed: 18076285]
13. Blitzblau HG, Bell GW, Rodriguez J, Bell SP, and Hochwagen A (2007). Mapping of meiotic single-stranded DNA reveals double-stranded-break hotspots near centromeres and telomeres. Current biology : CB 17, 2003–2012. [PubMed: 18060788]
14. Cartagena-Lirola H, Guerini I, Manfrini N, Lucchini G, and Longhese MP (2008). Role of the Saccharomyces cerevisiae Rad53 checkpoint kinase in signaling double-strand breaks during the meiotic cell cycle. Molecular and cellular biology 28, 4480–4493. [PubMed: 18505828]
15. Lydall D, Nikolsky Y, Bishop DK, and Weinert T (1996). A meiotic recombination checkpoint controlled by mitotic checkpoint genes. Nature 383, 840–843. [PubMed: 8893012]
16. Sanchez Y, Desany BA, Jones WJ, Liu Q, Wang B, and Elledge SJ (1996). Regulation of RAD53 by the ATM-like kinases MEC1 and TEL1 in yeast cell cycle checkpoint pathways. Science 271, 357–360. [PubMed: 8553072]
17. Cohen-Fix O, and Koshland D (1997). The anaphase inhibitor of Saccharomyces cerevisiae Pds1p is a target of the DNA damage checkpoint pathway. Proc Natl Acad Sci U S A 94, 14361–14366. [PubMed: 9405617]

18. Sanchez Y, Bachant J, Wang H, Hu F, Liu D, Tetzlaff M, and Elledge SJ (1999). Control of the DNA damage checkpoint by chk1 and rad53 protein kinases through distinct mechanisms. Science 286, 1166–1171. [PubMed: 10550056]
19. Wang H, Liu D, Wang Y, Qin J, and Elledge SJ (2001). Pds1 phosphorylation in response to DNA damage is essential for its DNA damage checkpoint function. Genes Dev 15, 1361–1372. [PubMed: 11390356]
20. Palou G, Palou R, Zeng F, Vashisht AA, Wohlschlegel JA, and Quintana DG (2015). Three Different Pathways Prevent Chromosome Segregation in the Presence of DNA Damage or Replication Stress in Budding Yeast. PLoS Genet 11, e1005468. [PubMed: 26332045]
21. Falk JE, Chan AC, Hoffmann E, and Hochwagen A (2010). A Mec1- and PP4-dependent checkpoint couples centromere pairing to meiotic recombination. Developmental cell 19, 599–611. [PubMed: 20951350]
22. Scarfone I, and Piatti S (2015). Coupling spindle position with mitotic exit in budding yeast: The multifaceted role of the small GTPase Tem1. Small GTPases 6, 196–201. [PubMed: 26507466]
23. D'Aquino KE, Monje-Casas F, Paulson J, Reiser V, Charles GM, Lai L, Shokat KM, and Amon A (2005). The protein kinase Kin4 inhibits exit from mitosis in response to spindle position defects. Mol Cell 19, 223–234. [PubMed: 16039591]
24. Pereira G, and Schiebel E (2005). Kin4 kinase delays mitotic exit in response to spindle alignment defects. Mol Cell 19, 209–221. [PubMed: 16039590]
25. Falk JE, Tsuchiya D, Verdaasdonk J, Lacefield S, Bloom K, and Amon A (2016). Spatial signals link exit from mitosis to spindle position. Elife 5.
26. Attner MA, Miller MP, Ee LS, Elkin SK, and Amon A (2013). Polo kinase Cdc5 is a central regulator of meiosis I. Proc Natl Acad Sci U S A 110, 14278–14283. [PubMed: 23918381]
27. Weinert TA, Kiser GL, and Hartwell LH (1994). Mitotic checkpoint genes in budding yeast and the dependence of mitosis on DNA replication and repair. Genes Dev 8, 652–665. [PubMed: 7926756]
28. Zhao X, Muller EG, and Rothstein R (1998). A suppressor of two essential checkpoint genes identifies a novel protein that negatively affects dNTP pools. Mol Cell 2, 329–340. [PubMed: 9774971]
29. White EJ, Cowan C, Cande WZ, and Kaback DB (2004). In vivo analysis of synaptonemal complex formation during yeast meiosis. Genetics 167, 51–63. [PubMed: 15166136]
30. Scherthan H, Wang H, Adelfalk C, White EJ, Cowan C, Cande WZ, and Kaback DB (2007). Chromosome mobility during meiotic prophase in Saccharomyces cerevisiae. Proc Natl Acad Sci U S A 104, 16934–16939. [PubMed: 17939997]
31. Straight AF, Marshall WF, Sedat JW, and Murray AW (1997). Mitosis in living budding yeast: anaphase A but no metaphase plate. Science 277, 574–578. [PubMed: 9228009]
32. Yaakov G, Thorn K, and Morgan DO (2012). Separase biosensor reveals that cohesin cleavage timing depends on phosphatase PP2A(Cdc55) regulation. Developmental cell 23, 124–136. [PubMed: 22814605]
33. Haruki H, Nishikawa J, and Laemmli UK (2008). The anchor-away technique: rapid, conditional establishment of yeast mutant phenotypes. Mol Cell 31, 925–932. [PubMed: 18922474]
34. Goyon C, and Lichten M (1993). Timing of molecular events in meiosis in Saccharomyces cerevisiae: stable heteroduplex DNA is formed late in meiotic prophase. Molecular and cellular biology 13, 373–382. [PubMed: 8417336]
35. Padmore R, Cao L, and Kleckner N (1991). Temporal comparison of recombination and synaptonemal complex formation during meiosis in S. cerevisiae. Cell 66, 1239–1256. [PubMed: 1913808]
36. Gasior SL, Wong AK, Kora Y, Shinohara A, and Bishop DK (1998). Rad52 associates with RPA and functions with rad55 and rad57 to assemble meiotic recombination complexes. Genes Dev 12, 2208–2221. [PubMed: 9679065]
37. Lao JP, Oh SD, Shinohara M, Shinohara A, and Hunter N (2008). Rad52 promotes postinvasion steps of meiotic double-strand-break repair. Mol Cell 29, 517–524. [PubMed: 18313389]
38. Lisby M, Rothstein R, and Mortensen UH (2001). Rad52 forms DNA repair and recombination centers during S phase. Proc Natl Acad Sci U S A 98, 8276–8282. [PubMed: 11459964]

39. Keeney S, Giroux CN, and Kleckner N (1997). Meiosis-specific DNA double-strand breaks are catalyzed by Spo11, a member of a widely conserved protein family. Cell 88, 375–384. [PubMed: 9039264]
40. Robinett CC, Straight A, Li G, Willhelm C, Sudlow G, Murray A, and Belmont AS (1996). In vivo localization of DNA sequences and visualization of large-scale chromatin organization using lac operator/repressor recognition. J Cell Biol 135, 1685–1700. [PubMed: 8991083]
41. Baro B, Queralt E, and Monje-Casas F (2017). Regulation of Mitotic Exit in Saccharomyces cerevisiae. Methods Mol Biol 1505, 3–17. [PubMed: 27826852]
42. Marston AL, Lee BH, and Amon A (2003). The Cdc14 phosphatase and the FEAR network control meiotic spindle disassembly and chromosome segregation. Developmental cell 4, 711–726. [PubMed: 12737806]
43. Buonomo SB, Rabitsch KP, Fuchs J, Gruber S, Sullivan M, Uhlmann F, Petronczki M, Toth A, and Nasmyth K (2003). Division of the nucleolus and its release of CDC14 during anaphase of meiosis I depends on separase, SPO12, and SLK19. Developmental cell 4, 727–739. [PubMed: 12737807]
44. Pereira G, Hofken T, Grindlay J, Manson C, and Schiebel E (2000). The Bub2p spindle checkpoint links nuclear migration with mitotic exit. Mol Cell 6, 1–10. [PubMed: 10949022]
45. Bardin AJ, Visintin R, and Amon A (2000). A mechanism for coupling exit from mitosis to partitioning of the nucleus. Cell 102, 21–31. [PubMed: 10929710]
46. Attner MA, and Amon A (2012). Control of the mitotic exit network during meiosis. Mol Biol Cell 23, 3122–3132. [PubMed: 22718910]
47. Wang Y, Hu F, and Elledge SJ (2000). The Bfa1/Bub2 GAP complex comprises a universal checkpoint required to prevent mitotic exit. Current biology : CB 10, 1379–1382. [PubMed: 11084339]
48. Geymonat M, Spanos A, Smith SJ, Wheatley E, Rittinger K, Johnston LH, and Sedgwick SG (2002). Control of mitotic exit in budding yeast. In vitro regulation of Tem1 GTPase by Bub2 and Bfa1. J Biol Chem 277, 28439–28445. [PubMed: 12048186]
49. Hu F, Wang Y, Liu D, Li Y, Qin J, and Elledge SJ (2001). Regulation of the Bub2/Bfa1 GAP complex by Cdc5 and cell cycle checkpoints. Cell 107, 655–665. [PubMed: 11733064]
50. Janke C, Magiera MM, Rathfelder N, Taxis C, Reber S, Maekawa H, Moreno-Borchart A, Doenges G, Schwob E, Schiebel E, et al. (2004). A versatile toolbox for PCR-based tagging of yeast genes: new fluorescent proteins, more markers and promoter substitution cassettes. Yeast 21, 947–962. [PubMed: 15334558]

Highlights

- The DNA damage and spindle positions checkpoints maintain meiotic commitment
- Cells that lose meiotic commitment return to mitosis and become polyploid
- Many cells have Spo11-dependent DNA damage that persists into the meiotic divisions
- Both checkpoints prevent premature meiotic exit in the presence of a mitosis signal

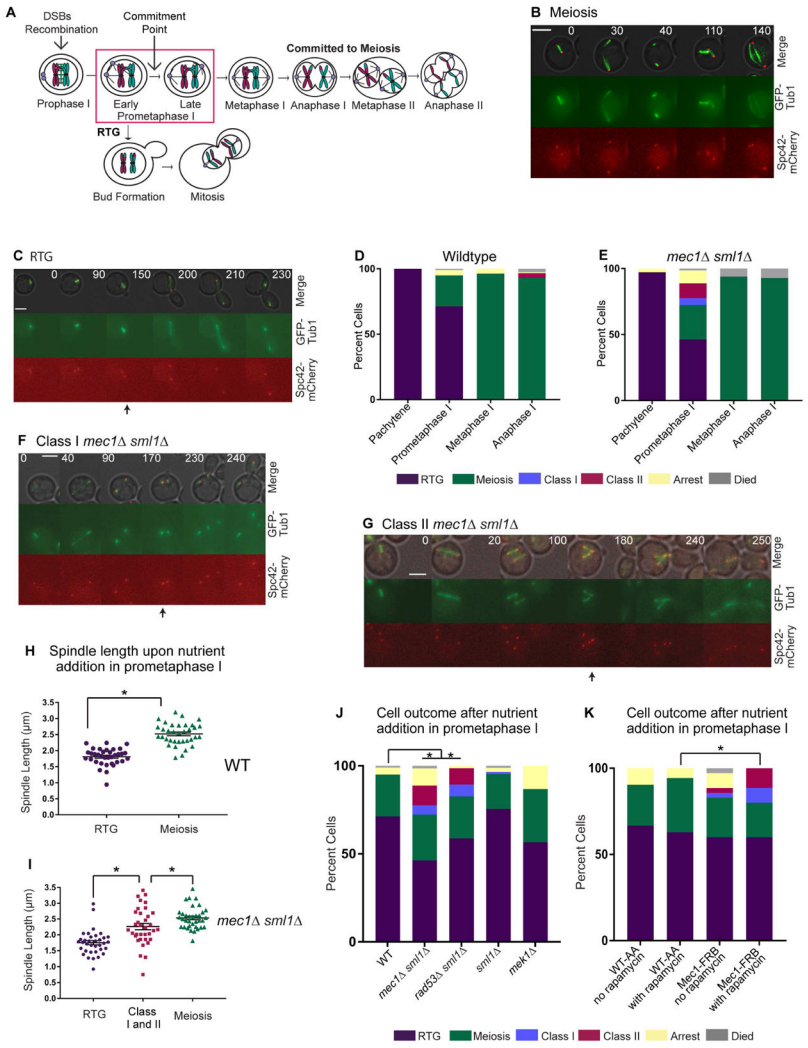

Figure 1. The DNA damage checkpoint prevents polyploidy upon RTG from prometaphase I.

(A) Cartoon of meiotic commitment. (B, C) Representative time-lapse images of a cell committed to meiosis (B) and underwent RTG (C) after nutrient-rich medium addition in prometaphase I. (D, E) Graph of the percentage of WT cells (D) and *mec1Δ sml1Δ* cells (E) with indicated outcomes upon nutrient-rich medium addition at each meiotic stage (n = 308 (D) and n=293 (E)). Three independent experiments were performed for each strain. (F, G) Representative time-lapse images of a cell that displayed the class I (F) and class II (G) phenotype. (H, I) Plot of spindle length (μm) at time of nutrient-rich medium addition in prometaphase I of wildtype (H) and *mec1Δ sml1Δ* (I) cells. Cells were categorized by outcome and corresponding spindle length (n = 35 for each category). Error bars represent SEM (standard error of the mean). (J, K) Graph of the percentage of cells for each outcome upon nutrient-rich medium addition during prometaphase I in indicated mutants ((n ≥ 50 prometaphase I cells for each mutant (J) and n ≥ 35 prometaphase I cells for each mutant (K), three independent experiments for each strain)). Asterisks indicate a statistically significant difference (H, I $p < 0.05$, Mann-Whitney Test) (J, K $p < 0.05$ rx Contingency Table). In all time-lapses (B, C, F, G), Cells expressed GFP-Tub1 and Spc42-mCherry.

Numbers indicate time (mins) from nutrient-rich medium addition at prometaphase I. Scale Bars: 5μm. Arrows indicate time of bud emergence. See also Figure S1.

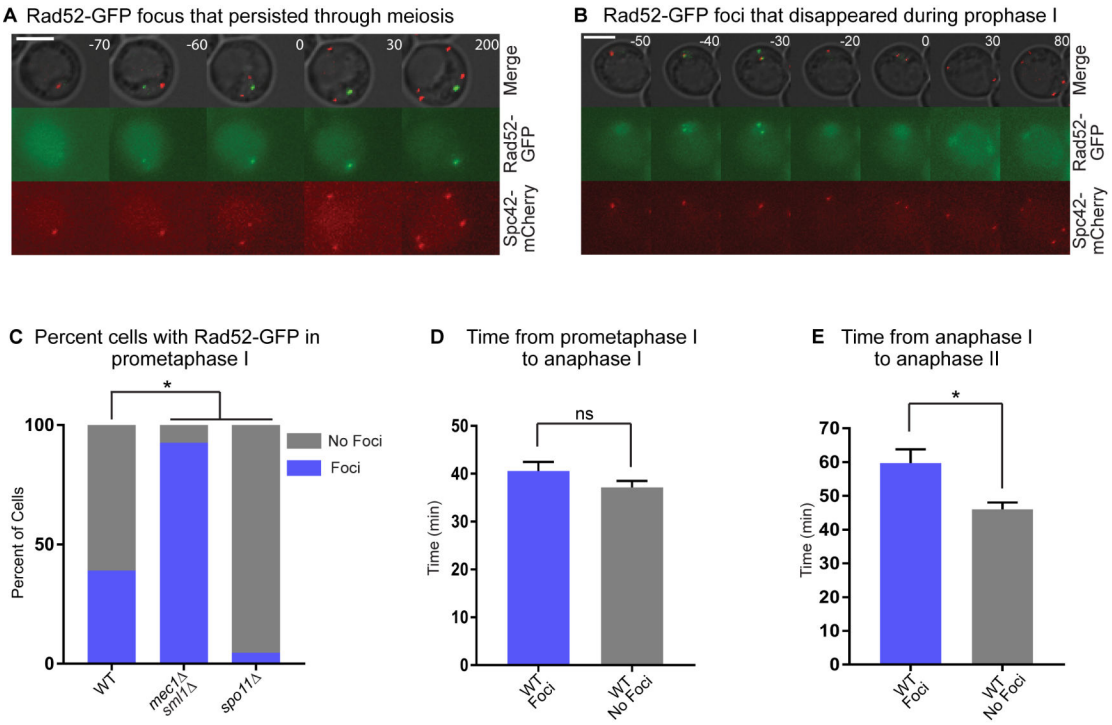

Figure 2. Persistent DSBs cause a DNA damage checkpoint delay in meiosis II

(A, B) Representative time-lapse images of a wildtype (WT) cell with a Rad52-GFP focus that persisted throughout the meiotic divisions (A), or a Rad52-GFP focus that disappeared during prophase I (B). Cells also expressed Spc42-mCherry. Numbers indicate time (mins) relative to prometaphase I initiation (spindle pole body separation). Scale Bars: 5μm. (C) Graph of percentage of wildtype, *mec1Δ sml1Δ,* and *spo11Δ* cells in meiosis with Rad52-GFP foci in prometaphase I ($n \geq 48$ cells for each). Three independent experiments performed for each strain. (D, E) Graph of the average time (mins) from prometaphase I to anaphase I (D), and anaphase I to anaphase II (E) in wildtype cells with or without Rad52-GFP foci in prometaphase I. Error bars represent SEM. ($n \geq 44$ cells). Asterisks indicate a statistically significant difference (C, $p < 0.0001$, Fisher's Exact Test) (D, E $p < 0.05$, Mann-Whitney test). ns represents not significant.

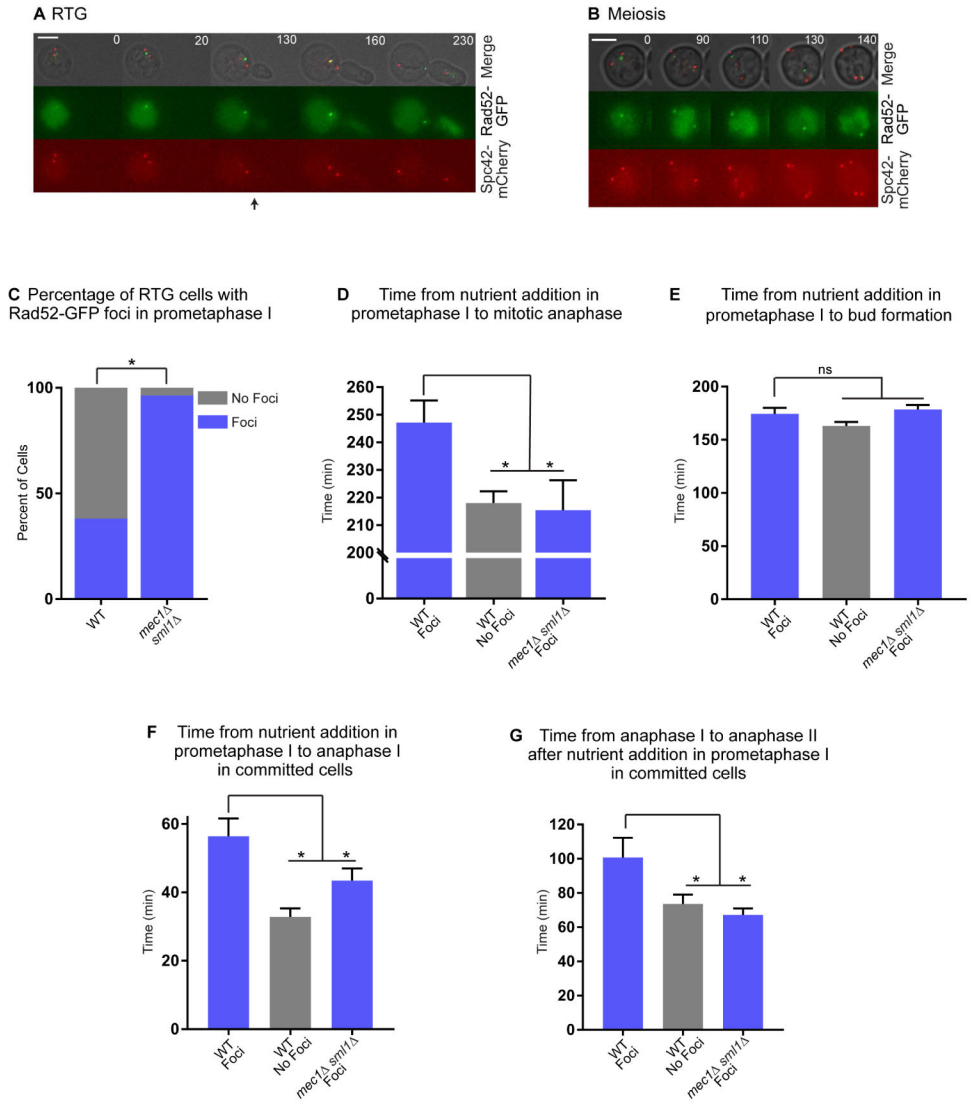

Figure 3. Cells with persistent Rad52-GFP that undergo RTG from prometaphase I have a DNA damage checkpoint delay

(A, B) Representative time-lapse images of a cell that underwent RTG (A), and finished meiosis (B) after nutrient-rich medium addition in prometaphase I. Cells expressed Rad52-GFP and Spc42-mCherry. Numbers indicate time (mins) from nutrient-rich medium addition in prometaphase I. Scale bars: 5μm. Arrow indicates time of bud emergence. (C) Graph of the percentage of WT and *mec1Δ sml1Δ* cells that underwent RTG from prometaphase I with Rad52-GFP foci ($n \geq 35$ cells). Three independent experiments performed for each strain. (D-G) Graph of average time (mins) from nutrient-rich medium addition in prometaphase I to mitotic anaphase (D), bud formation (E), anaphase I (F), or from anaphase I to anaphase II (G) in WT and *mec1Δ sml1Δ* cells with Rad52-GFP foci in prometaphase I ($n = 35$). Error bars represent SEM. Asterisks indicate a statistically significant difference from WT (D-G, $p < 0.05$, Mann-Whitney Test) (C, $p < 0.0001$, Fisher's Exact Test). ns represents not significant.

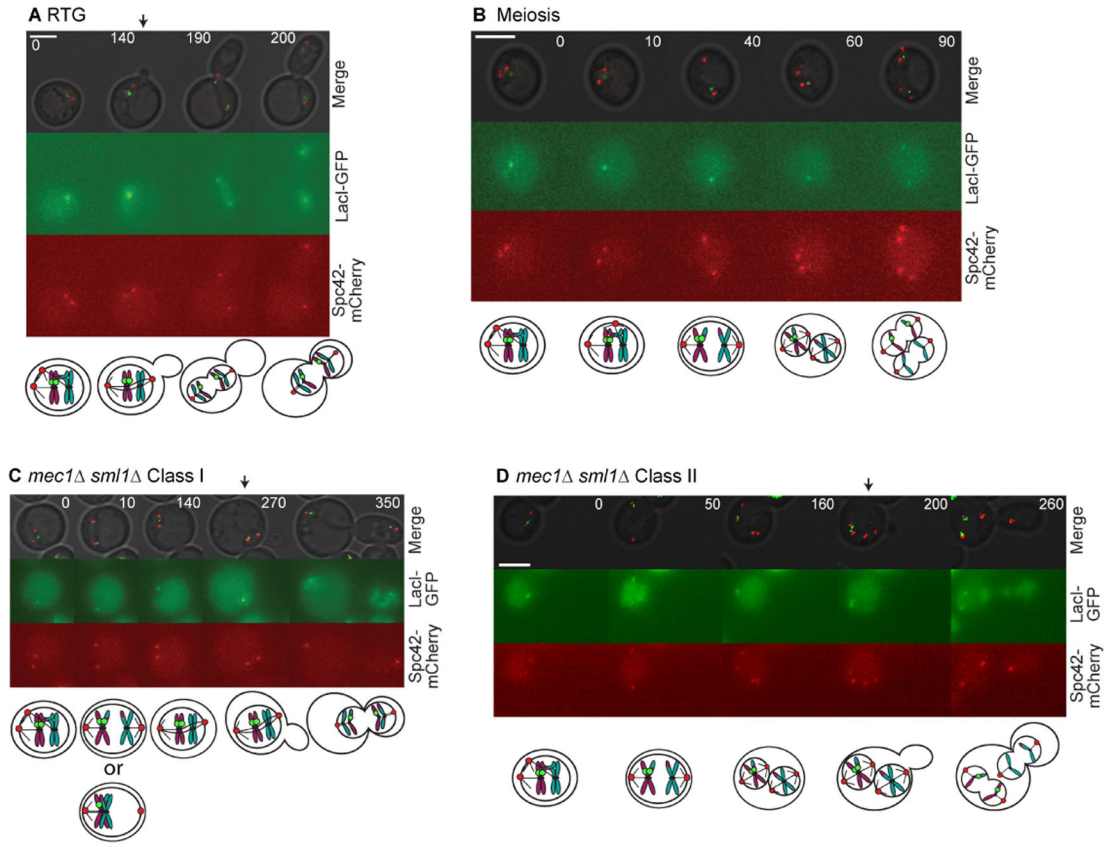

Figure 4. Class I and class II *mec1Δ sml1Δ* cells segregate homologous chromosomes in the first division

(A-D) Representative time-lapse images and cartoons of a cell that underwent RTG (A) finished meiosis (B) displayed the class I (C) and class II phenotype (D) ((n=50 cells for (A) and (B) and n=10 cells for (C) and (D)). Cells expressed LacI-GFP and Spc42-mCherry. Numbers indicate time (mins) from nutrient-rich medium addition at prometaphase I. Scale bars: 5μm. Arrows indicate time of bud emergence.

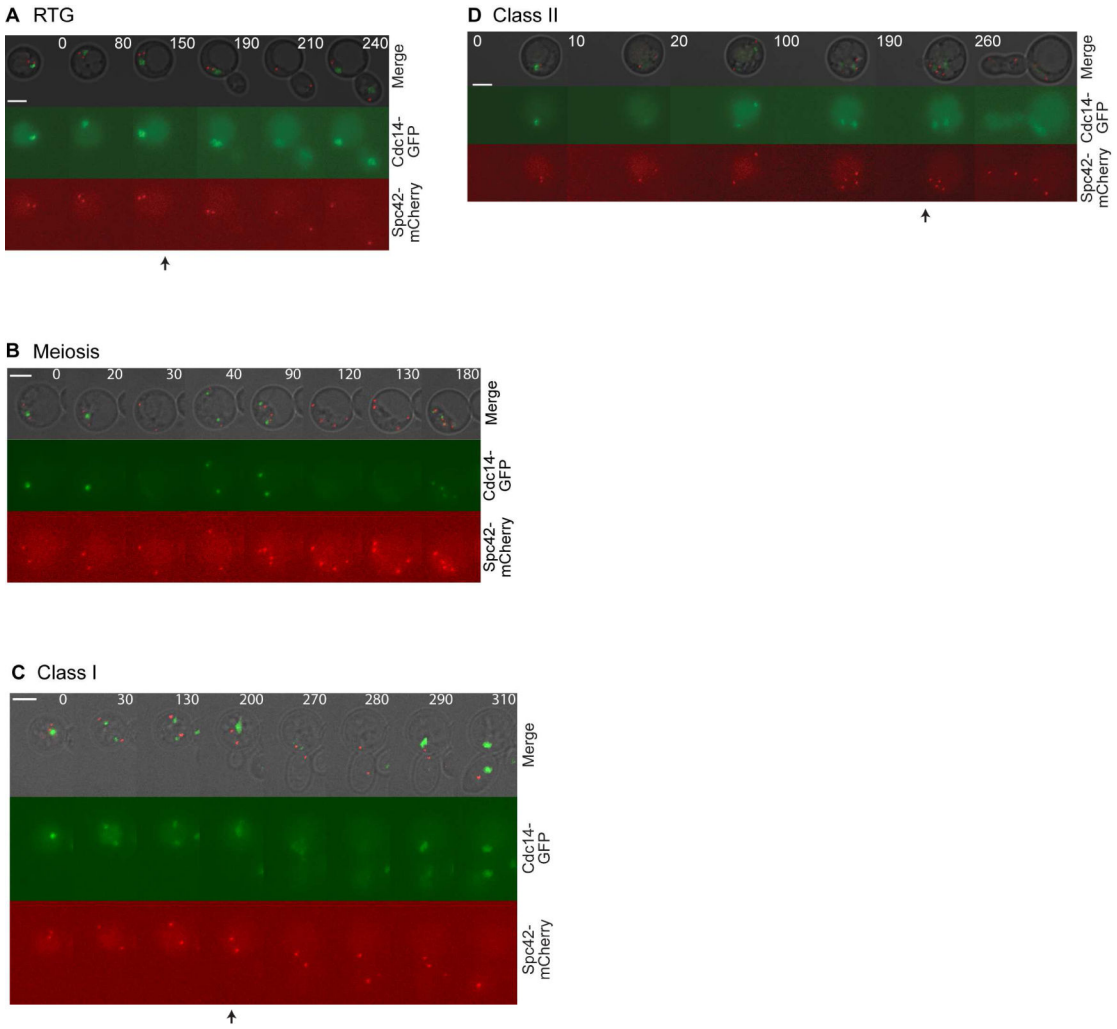

Figure 5. The spindle position checkpoint delays Cdc14 release in Class I cells.

(A-D) Representative time-lapse images of a cell that underwent RTG (A), finished meiosis (B), displayed the class I phenotype (C), and class II phenotype (D) upon nutrient-rich medium addition in prometaphase I. Cells expressed Cdc14-GFP and Spc42-mCherry. Numbers indicate time (mins) from nutrient-rich medium addition at prometaphase I. Scale bars: 5μm. Arrows indicate time of bud emergence. See also Figure S2.

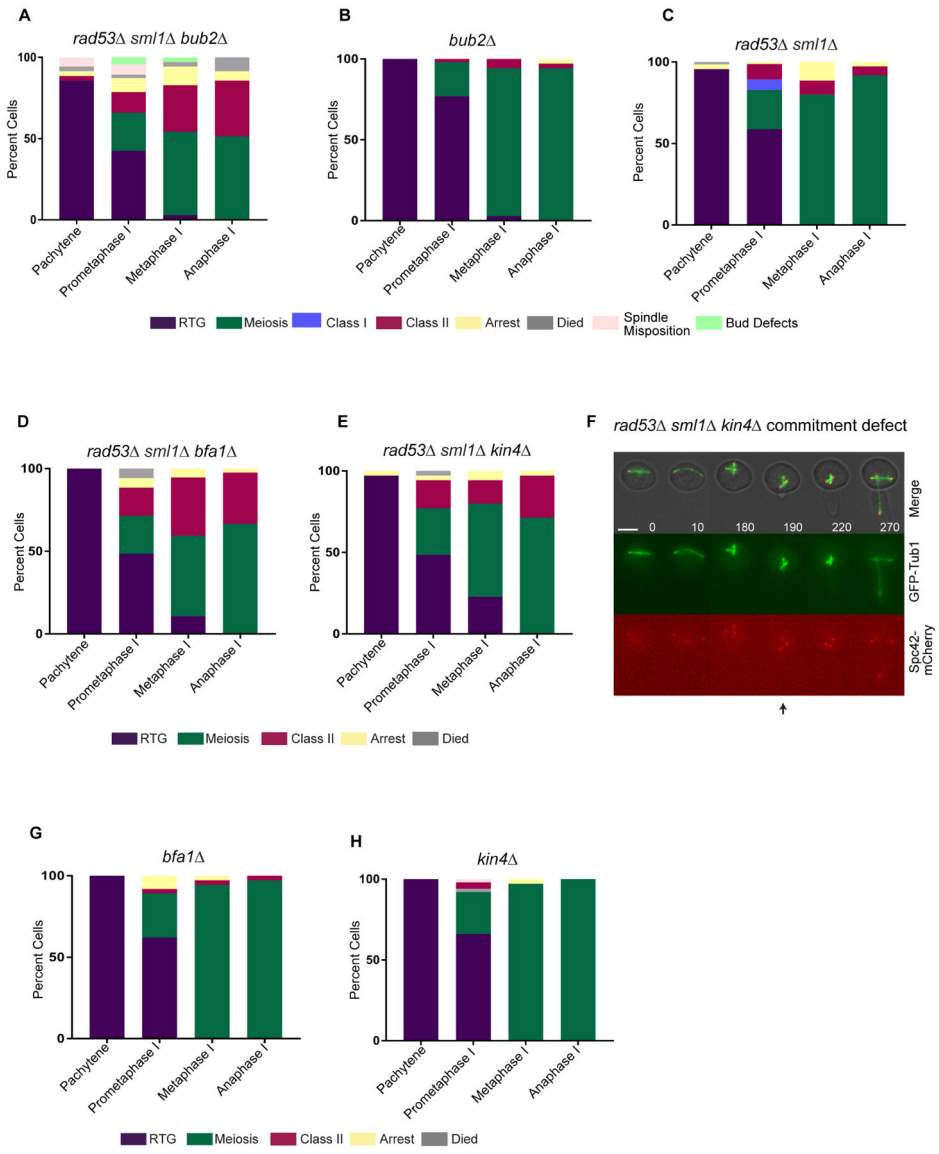

Figure 6. Cells fail to stay committed to meiosis in the absence of both the DNA damage checkpoint and spindle position checkpoint.

(A-E, G, H) Graph of percentage of *rad53Δ sml1Δ bub2Δ* (A), *bub2Δ* (B), *rad53Δ sml1Δ* (C), *rad53Δ sml1Δ bfa1Δ* (D), and *rad53Δ sml1Δ kin4Δ* (E), *bfa1Δ* (G), and *kin4Δ* cells (H), with indicated outcomes upon nutrient-rich medium addition at each meiotic stage ((n= 152 (A), n=157 (B), n=216 (C), n=149 (D), n=140 (E), n=145 (G) and n=158 (H)). Two or more independent experiments performed for each strain. (*rad53Δ sml1Δ kin4Δ, rad53Δ sml1Δ bfa1Δ,* and *rad53Δ sml1Δ bub2Δ* all displayed a statistically significant difference from wildtype in prometaphase I, metaphase I, and anaphase I. The above mutants were also significantly different from the corresponding single mutant (*kin4Δ, bfa1Δ,* and *bub2Δ,* respectively) in prometaphase I, metaphase I, and anaphase I ($p < 0.01$, rx Contingency Tables)). (F) Representative time-lapse images of a *rad53Δ sml1Δ kin4Δ* cell expressing GFP-Tub1 and Spc42-mCherry that is uncommitted. Numbers indicate time (mins) from

nutrient-rich medium addition at anaphase I. Scale bar: 5mm. Arrow indicates time of bud emergence. See also Figure S3.